

Analysis, Modeling and Implementation of a Switching Bi-Directional Buck-Boost Converter Based on Electric Vehicle Hybrid Energy Storage for V2G System

P.Lakshmi Priyanka
Assistant Professor

Dept.of Electrical and Electronics Engineering
Anantha Lakshmi Institute of Technology and
Sciences, Ananthapuramu.

P.Janardhan Guptha
Assistant Professor

Dept.of Electrical and Electronics Engineering
Anantha Lakshmi Institute of Technology and
Sciences, Ananthapuramu

ABSTRACT

This paper presents a switching bi-directional buck-boost converter (SBBBC) for vehicles to-grid (V2G) system. The topology can provide an energy bi-directional flow path for energy exchange between the Li-battery/super capacitor (SC) hybrid energy storage system (HESS) of the electric vehicle and the grid. This topology not only has buck-boost capability, but also has the function of energy management. In this paper, the state-space averaging method is used to analyze the stability of the topology in boost and buck modes. The control strategy is given according to the state of charge (SOC) of the energy storage system to ensure that the output voltage and current are stable. And the Li-battery is charged in constant current (CC) and constant voltage (CV) mode. The voltage and current controllers are designed in the frequency domain based on bode plots. Finally, the electrical feasibility of the topology, the suitability of the design controller and control strategy are verified by simulation and experiment.

INTRODUCTION

Electric vehicles have been widely used because of their cleanliness and low impact on the environment [1]. Li-batteries are of critical importance part in energy storage systems of electric vehicle [2]. Although Li-batteries with high energy densities can provide enough energy during steady-state operation, the power densities of Li-batteries are too low to meet the peak power demand [3], [4]. Combining Li-batteries and super capacitors (SC) to form a hybrid energy storage system (HESS) can solve

the problem. The reason is that SC with higher power densities can provide the transient power required.

Since output voltage peak of the voltage source inverter is less than the dc-link side voltage, it is necessary to use the dc-dc converter to raise the Li-battery voltage [18].

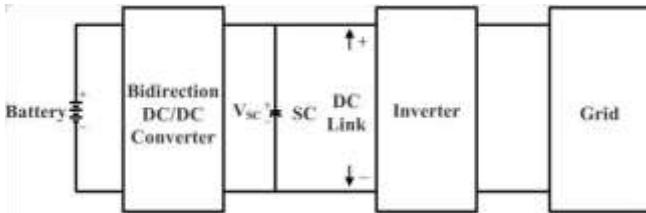


FIGURE 1. The block diagram of HESS.

The SC is directly connected to the inverter, which can increase the dynamic response of the HESS during transient peak power demand, while the Li-battery is connected to the DC-link by a bi-directional DC/DC converter [19]. The effect of the bi-directional dc-dc converter in the HESS is to transfer the energy and keep the dc bus voltage stability. Moreover, the converter should provide bi-directional power flow because the energy storage system and the grid require energy HESS topology is mentioned in articles [3] and [5].

In the topology of [3] and [5], the Li-battery can be connected to the SC via a bi-directional dc-dc half-bridge or directly to the DC bus via a diode. This two-stage converter can make full use of the power capacity of the SC but the boost ratio is low. A buck-boost converter for a plug-in hybrid electric vehicle is proposed in paper [21] and [22], respectively. However, the converter mentioned in the paper [21] cannot achieve a bidirectional flow of energy between the grid and the energy storage device. The converter mentioned in the paper [22] has many switching devices, large losses and complicated control. A high voltage gain bi-directional dc-dc converter is given in article [23]. This topology can operate

under zero voltage switching conditions and reduces switching and conduction losses. However, this topology has many switching states and the operation is complicated.

In [13] and [24], hybrid energy storage systems for electric vehicles based on Z-source inverters (ZSI) and quasi-Z- source inverters (qZSI) were proposed. These two topologies have the boost capability, and provide a bi-directional energy flow path. Moreover, the reliability of the hybrid energy storage system is enhanced due to the characteristics that allow the inverter to shoot-through. These two topologies can increase power density [25]. The control strategies proposed in [13] and [24] are complex, and the topologies have multiple passive components between the SC and the DC bus, which will greatly increase the size of the device.

This paper proposes a switching bi-directional buck-boost converter (SBBBC) and its appropriate control strategy, which is used in the HESS for vehicles-to-grid (V2G) system. The converter allows shoot-through of two switches of any phase, with anti-electromagnetic interference capability. Meanwhile, since there are three switches in the DC side, the SC and Li-battery can fulfill bi-directional power flow. Furthermore, the small-signal model of the topology is established by state space averaging method and the stability of the system is analyzed. The control strategy is given according to the state of charge (SOC) of the energy storage system and the operating state of the circuit. The performance of the proposed converter and control strategy are verified through simulation and experimental results.

and complementary to the gate signal of switch $SD1$, one gate signal can control these three additional switches. This unique SBBBC network allows the

TOPOLOGY AND MODULATION OF THE PROPOSED SWITCHING BI-DIRECTION BUCK-BOOST CONVERTER

A. PROPOSED TOPOLOGY

Figure 2 shows the proposed SBBBC with HESS, which consists of five parts: Li-battery, switching bi-directional buck-boost circuit, SC, full bridge inverter and grid. The switching bi-directional buck-boost circuit has an inductor, SC and the additional three switches ($SD1$, $SD2$, $SD3$). Since the gate signals of switches $SD2$ and $SD3$ are the same

system work on the buck and boost modes, and it can provide bi-directional power flow.

FIGURE 2. The proposed SBBBC.

TABLE 1. Switch combination and inverter output voltage.

MODULATION METHOD

In the proposed converter, there are three switching-states include active state, zero state and shoot-through state respectively, as shown in Table 1. All switches of full bridge inverter are operated in the SPWM mode to modulate output voltage. The switching bi-directional buck-boost circuit uses the shoot-through duty to achieve buck-boost voltage.

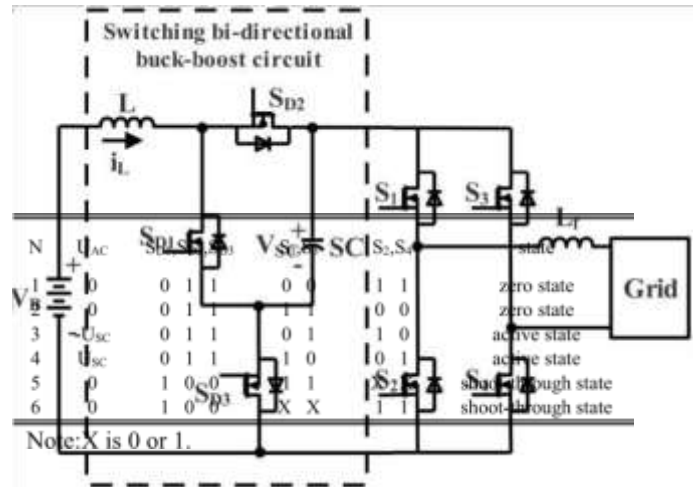
The duty cycle is calculated by:

$$d = m \sin(\theta)$$

$$d_s = \text{const} \quad (d_s \leq 1)$$

$$-d) d_0 = 1 - d - d_s$$

where m is the modulation index of the inverter; θ is the vector angle of the output voltage; d , d_s , d_0 are the duty cycles of the output voltage active state, shoot-through state and zero voltage state, respectively.



**MODELING AND ANALYSIS OF THE
 PROPOSED CONVERTER**

FIGURE 4. Flow path in active state of boost mode.

The proposed Converter can provide bi-directional power flow among SC, Li-battery and grid, as shown in Figure 2. And the converter can work in boost mode and buck mode.

BOOST MODE

During boost mode, the proposed converter boosts the low Li-battery voltage to high dc-link voltage. There are three work states: zero state, active state and shoot-through state.

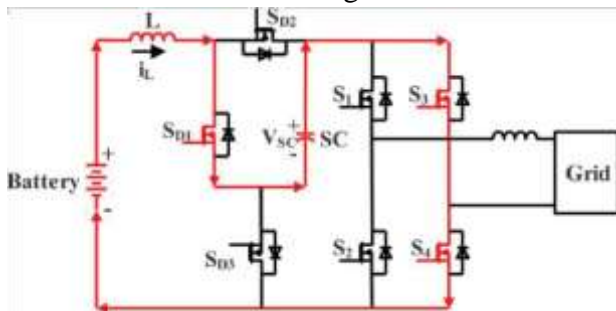


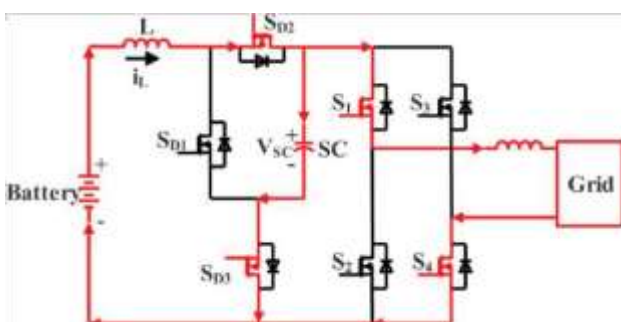
FIGURE 3. Flow path in shoot-through state of boost mode.

SHOOT-THROUGH STATE

In shoot-through state, the switches *SD1* and *S3* & *S4* (*S1* & *S2*) are turned ON while switches *SD2* and *SD3* are simultaneously turned OFF, as shown in Figure 3. In this state, the power is transferred from the Li-battery and SC to the inductor *L*.

ACTIVE STATE

In active state, both switches *SD2* and *SD3* are turned ON while switches *SD1* is simultaneously turned OFF, as shown in Figure 4. In this state, the Li-battery *VB* and inductor *L* charge SC and power is transferred from the Li-battery *VB* and inductor *L* to the grid.



ZERO STATE

In zero state, both switches $SD2$ and $SD3$ and $S1$ & $S3$ ($S2$ & $S4$) are turned ON while switches $SD1$ is simultaneously.

FIGURE 5. Flow path in zero state of boost mode.

BUCK MODE

In buck mode, energy is transferred from the AC side to the DC side, and the single-phase full bridge converter operates in the rectification mode. Therefore, the dc link voltage is higher than the input AC voltage.

ACTIVE STATE AND ZERO STATE

In active state and zero state, the switches $SD2$ and $SD3$ are turned ON while switch $SD1$ is simultaneously turned OFF, as shown in Figure 7. In this state, the voltage of the DC bus is equal to the SC voltage, and power is transferred from the dc link to the Li-battery and inductor.

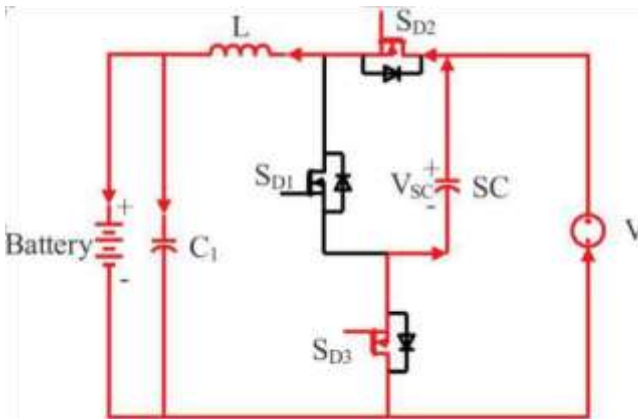
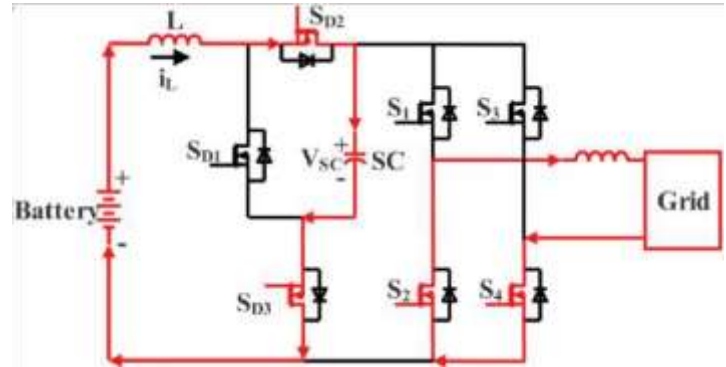


FIGURE 6. Flow path in active state and zero state of buckmode.

SHOOT-THROUGH STATE

In shoot-through state, the switches $SD1$ and $S3$ & $S4$ ($S1$ & $S2$) are turned ON while switches $SD2$ and $SD3$ are simultaneously turned OFF, as shown in Figure 8. In this state, the inductor L charges SC and Li-battery VB . The power is transferred from inductor L to the Li-battery VB and SC.

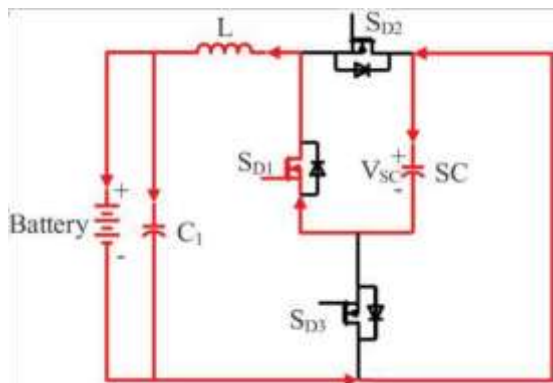


FIGURE 8. Flow path in shoot-through state of buck mode.

CONTROL STRATEGY AND CONTROLLER DESIGN

CONTROL STRATEGY

The control strategy diagram of the proposed converter is shown in Figure 12. The control scheme includes four controllers. The SC voltage controller PI1 outputs a duty cycle $d1$ for controlling the SC voltage. The Li-battery current controller PI2 and the Li-battery voltage controller PI3 are two parallel controllers for controlling the charging current and voltage of the Li-battery. The controller PI2 outputs a duty cycle $d2$, and the controller PI3 outputs a duty cycle $d3$. The grid current controller PR outputs a duty cycle $d4$. The PR controller can track the sinusoidal reference of the grid current [32]. The proposed control strategy has two operation modes which are vehicles-to-grid (V2G) and grid- to vehicles (G2V).

V2G MODE

In V2G mode, the flow chart of the control strategy is shown in Figure 13. The Li-battery and SC work together to supply the grid. When the required power of the grid PG is equal to or less

than the rated power of the Li-battery PB . The energy required by the grid is mainly provided by the Li-battery. In this case, the $d1$ obtains control

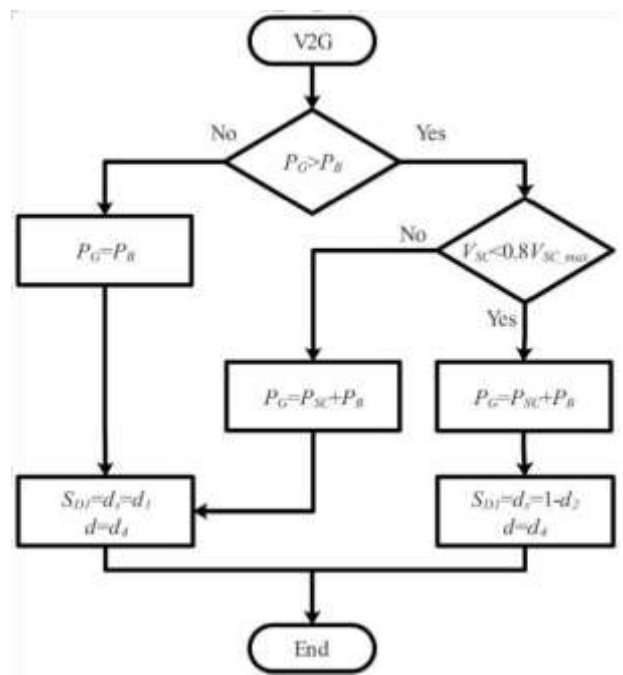
of the shoot-through state duty cycle d_s , and the d_4 obtains control of the active state duty cycle d . In the stage of increased grid load, the power demand of the grid is higher than the Li-battery rated power. The SC meets the peak power demand of the grid in this condition. When the SC voltage is higher than $0.8V_{SC_max}$, the voltage controller PI1 works. When the SC voltage is lower than $0.8V_{SC_max}$, the d_2 obtains control of the shoot-through state duty cycle d_s .

The energy stored in the capacitor depends on the voltage of the capacitor [3]:

$$E_c = \frac{1}{2} CV^2$$

From equation (28), when the capacitor voltage VC is charged to 50% of the maximum voltage of the capacitor VC_max , the capacitor stores only 25% of the energy. If the voltage closed loop stabilizes the capacitor voltage at 80% of the capacitor's maximum voltage, the capacitor store 64% of the energy. The reason for choosing the 80% voltage charging ratio is that the DC bus voltage will not drop greatly when the capacitor supplies power to the grid, and there is enough capacity to achieve voltage regulation of the DC bus.

FIGURE 13. The flow chart of the control strategy in V2Gmode.



G2V MODE

mode.

In G2V mode, energy flows from the grid to HESS. The flowchart of the control strategy is shown in Figure 14. The Li- battery is charged from constant current (CC) mode to constant voltage (CV) mode. The smaller one of the d_2 and the d_3 can obtain the control of the shoot-through-duty ratio d_s . When the d_2 obtain the control of the shoot-through-duty ratio d_s , the charger charges the Li-battery with a constant current ICC . When the d_3 obtain the control of the shoot through-duty ratio d_s , the charger charges the Li-battery with a constant voltage VH .

The control block diagram of the Li-battery charger is shown in Figure 15. When the Li-battery voltage VB is lower than the reference voltage VH , d_3 is greater than d_2 , so d_2 obtains control of the duty cycle d_s . The SBBBC is controlled by the current closed loop and I_o traces to its reference ICC . At this time, the Li-battery voltage starts to rise. When the Li- battery voltage reaches the reference voltage VH , the charging current is less than the ICC . At this time d_2 is greater than d_3 , so d_3 obtains control of the duty cycle d_s . The SBBBC is controlled by the voltage closed loop and VB traces to its reference VH .

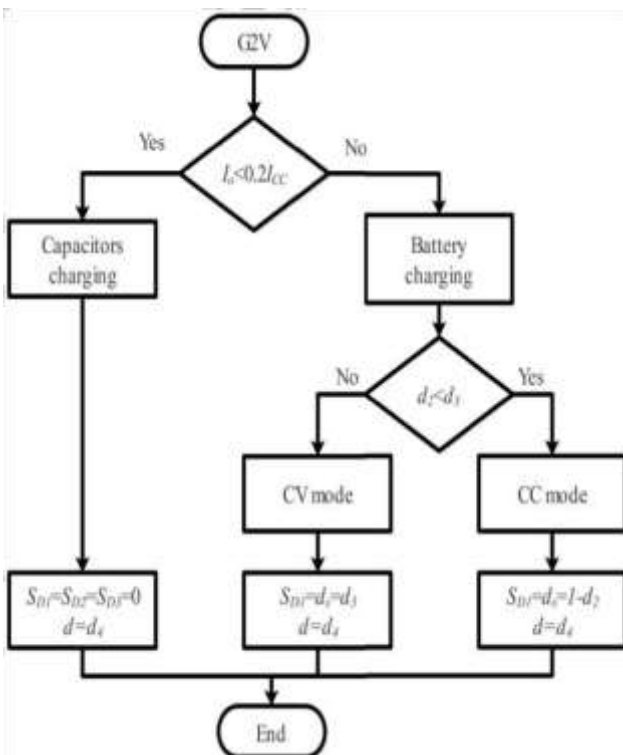


FIGURE 14. The flow chart of the control strategy in G2V

According to the transfer functions given in Section IV, the bode diagram can be used to design the PI controller in the frequency domain.

The bode plot of the current loop is shown in Figure 17 and the bode plot of the voltage loop in buck mode is shown in Figure 18. As shown in the open-loop bode plot of the voltage loop, the phase margin is 80.4 The phase margin of the open-loop bode plot of the current loop is 70. It can be seen that the system has a high stability margin. In order to obtain a good dynamic response, the appropriate cutoff frequency of the open-loop bode plot is 1kHz when the switching frequency of the converter is 10 kHz.

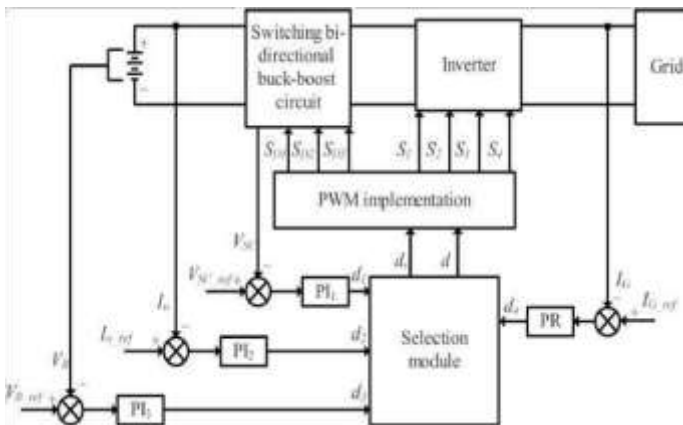


FIGURE 12. The control strategy diagram.

FIGURE 15. Control block diagram of a Li-battery charger.

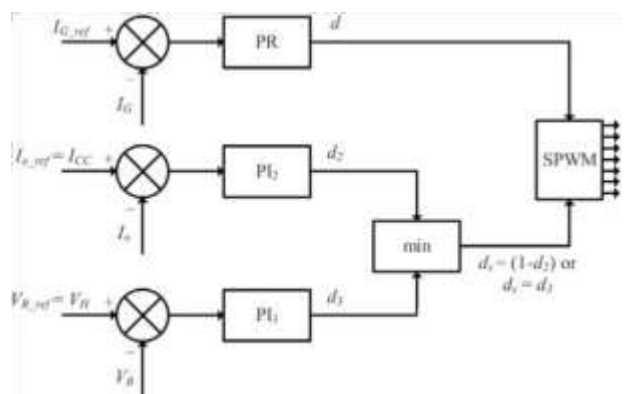


Figure 19 shows the simulation waveforms when the SBBBC is operating in boost mode. To make the grid current clear, the amplitude of the grid current is amplified 10 times. The current injected into the grid is in phase with the grid voltage to achieve a unit power factor. As shown in Figure19(b), when the shoot-through duty cycle d_S is 0.25, the proposed converter boosts the 100V Li-battery voltage to 200V SC voltage, which meets the voltage gain given by equation (5). At $t = 0.5$, the reference current IG_ref of

which can achieve a fast response of the grid current. The capacitor voltage remains constant and the energy required by the grid is

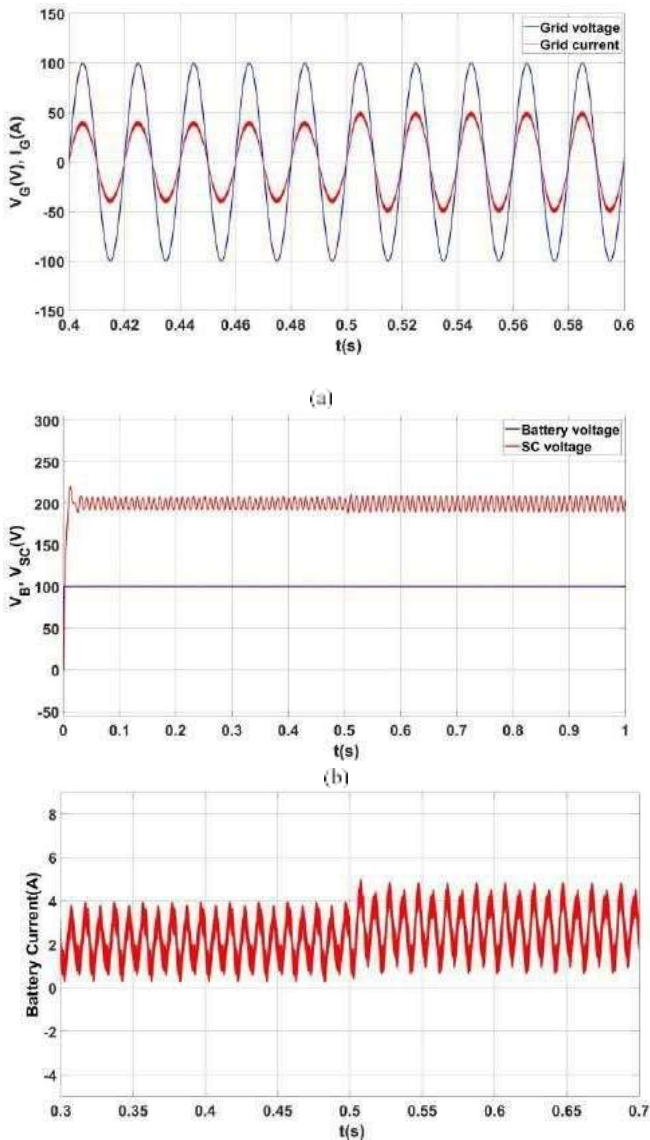


FIGURE 19. Simulation results of the proposed system. (a) Grid voltage and grid current. (b) Battery discharge voltage and SC voltage. (c) Battery discharge current.

the grid current controller changes from 4A to 5A. At this time, the Li-battery current increases and the output power of the Li-battery increases,

Figure 20 shows the main waveforms when the SBBBC is operating in buck mode. To make the grid current clear, the amplitude of the grid current is amplified by 10 times. The grid current is in reverse phase with the grid voltage, so the energy flows from the grid to the HESS. At this time, the grid charges the energy storage system. At $t = 0.5$, the amplitude of grid voltage drops from 100V to 95V. As shown in Figure 20(a), when the grid voltage decreases, the grid current can quickly reach a stable state under the action of the grid-connected controller. The Li-battery charging current waveform is shown in Figure 20(b). It can be seen that the charging current of the Li-battery remains constant. As shown in Figure 20(c), the SC outputs energy to the Li-battery.

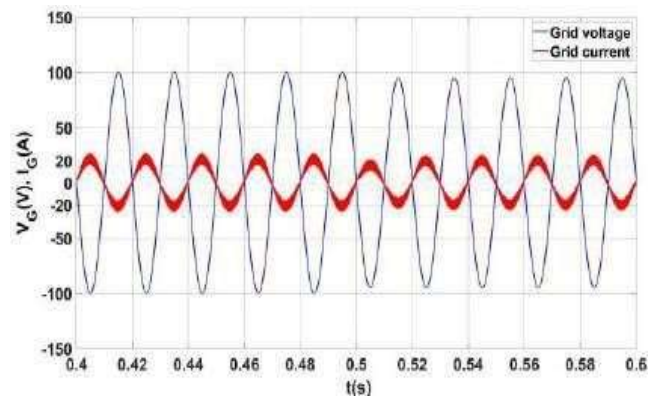
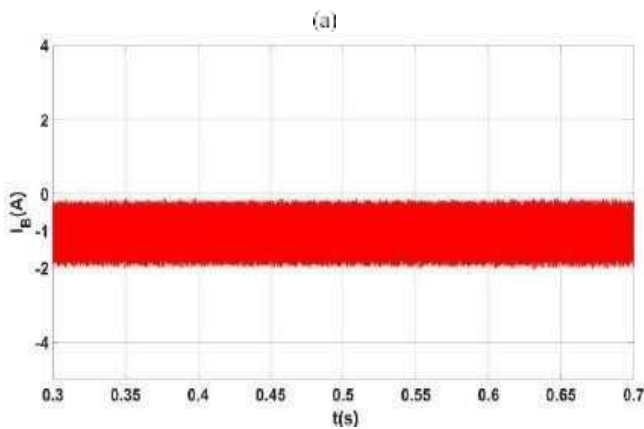
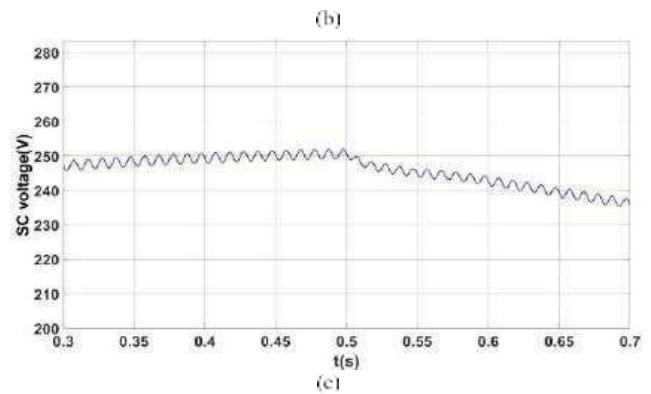


FIGURE 20. Simulation results of the proposed system.
(a) Grid voltage and grid current. (b) Battery charging current. (c) SC voltage.



CONCLUSION

This paper presents a SBBBC for V2G system. The proposed converter not only has high voltage gain and immunity to electromagnetic interference, but also provides a bi-directional energy flow path. In this paper, different working modes of the SBBBC are discussed in detail and the small signal model of the converter is established. The zero-pole diagram of the system was drawn, the dynamic characteristics of the system were analyzed and its stability was proved. This paper proposes control strategies for V2G and G2V modes, which implement energy management of the HESS. The controller is designed in the frequency domain, so that the controller has good dynamic performance. Finally, the correctness of the theory and the feasibility of the control strategy have been verified through simulations and experiments on laboratory prototypes.

REFERENCES

- [1] F. Naseri, E. Farjah, and T. Ghanbari, "An efficient regenerative braking system based on battery/supercapacitor for electric, hybrid and plug-in hybrid electric vehicles with BLDC motor," *IEEE Trans. Veh. Technol.*, vol. 66, no. 5, pp. 3724–3738, May 2017.
- [2] S. G. Wirasingha and A. Emadi, "Classification and review of control strategies for plug-in hybrid electric vehicles," *IEEE Trans. Veh. Technol.*, vol. 60, no. 1, pp. 111–122, Jan. 2011.
- [3] J. Cao and A. Emadi, "A new battery/ultraCapacitor hybrid energy storage system for electric, hybrid, and plug-in hybrid electric vehicles," *IEEE Trans. Power Electron.*, vol. 27, no. 1, pp. 122–132, Jan. 2012.
- [4] O. Hegazy, J. V. Mierlo, and P. Lataire, "Analysis, modeling, and implementation of a multidevice interleaved DC/DC converter for fuel cell hybrid electric vehicles," *IEEE Trans. Power Electron.*, vol. 27, no. 11, pp. 4445–4458, Nov. 2012.
- [5] A. Khaligh and Z. Li, "Battery, ultracapacitor, fuel cell, and hybrid energy storage systems for electric, hybrid electric, fuel cell, and plug-in hybrid electric vehicles: State of the art," *IEEE Trans. Veh. Technol.*, vol. 59, no.6, pp. 2806–2814, Jul. 2010.
- [6] M. Ortuzar, J. Moreno, and J. Dixon, "Ultracapacitor-based auxiliary energy system for an electric vehicle: Implementation and evaluation," *IEEE*

- Trans. Ind. Electron.*, vol. 54, no. 4, pp. 2147–2156, Aug. 2007.
- [7] L. Gao, R. A. Dougal, and S. Liu, “Power enhancement of an actively controlled battery/ultracapacitor hybrid,” *IEEE Trans. Power Electron.*, vol. 20, no. 1, pp. 236–243, Jan. 2005.
- [8] L. Solero, A. Lidozzi, and J. A. Pomilio, “Design of multiple-input power converter for hybrid vehicles,” *IEEE Trans. Power Electron.*, vol. 20, no. 5, pp. 1007–1016, Sep. 2005.
- [9] M.-E. Choi, S.-W. Kim, and S.-W. Seo, “Energy management optimization in a battery/supercapacitor hybrid energy storage system,” *IEEE Trans. Smart Grid*, vol. 3, no. 1, pp. 463–472, Mar. 2012.
- [10] J. Shen and A. Khaligh, “Design and real-time controller implementation for a battery-ultracapacitor hybrid energy storage system,” *IEEE Trans. Ind. Informat.*, vol. 12, no. 5, pp. 1910–1918, Oct. 2016.
- [11] Y. Ghiassi-Farrokhfal, C. Rosenberg, S. Keshav, and M.-B. Adjaho, “Joint optimal design and operation of hybrid energy storage systems,” *IEEE J. Sel. Areas Commun.*, vol. 34, no. 3, pp. 639–650, Mar. 2016.
- [12] Z. Song, H. Hofmann, J. Li, X. Han, and M. Ouyang, “Optimization for a hybrid energy storage system in electric vehicles using dynamic programming approach,” *Appl. Energy*, vol. 139, pp. 151–162, Feb. 2015.
- [13] S. Hu, Z. Liang, and X. He, “Ultracapacitor-battery hybrid energy storage system based on the asymmetric bidirectional Z-source topology for EV,” *IEEE Trans. Power Electron.*, vol. 31, no. 11, pp. 7489–7498, Nov. 2016.
- [14] N. Qi, K. Dai, F. Yi, X. Wang, Z. You, and J. Zhao, “An adaptive energy management strategy to extend battery lifetime of solar powered wireless sensor nodes,” *IEEE Access*, vol. 7, pp. 88289–88300, 2019.
- [15] Z. Amjadi and S. S. Williamson, “Power-electronics-based solutions for plug-in hybrid electric vehicle energy storage and management systems,” *IEEE Trans. Ind. Electron.*, vol. 57, no. 2, pp. 608–616, Feb. 2010.

- [16] C. Zheng, W. Li, and Q. Liang, "An energy management strategy of hybrid energy storage systems for electric vehicle applications," *IEEE Trans. Sustain. Energy*, vol. 9, no. 4, pp. 1880–1888, Oct. 2018.
- [17] H. H. Eldeeb, A. T. Elsayed, C. R. Lashway, and O. Mohammed, "Hybrid energy storage sizing and power splitting optimization for plug-in electric vehicles," *IEEE Trans. Ind. Appl.*, vol. 55, no. 3, pp. 2252–2262, May 2019.
- [18] J. Fang, Y. Tang, H. Li, and X. Li, "A battery/ultracapacitor hybrid energy storage system for implementing the power management of virtual synchronous generators," *IEEE Trans. Power Electron.*, vol. 33, no. 4, pp. 2820–2824, Apr. 2018.
- [19] C. Zhao, H. Yin, Z. Yang, and C. Ma, "Equivalent series resistance-based energy loss analysis of a battery semiactive hybrid energy storage system," *IEEE Trans. Energy Convers.*, vol. 30, no. 3, pp. 1081–1091, Sep. 2015.
- [20] M.A.Khan,A.Ahmed,I.Husain,Y.Sozer,and M.Badawy,"Performance analysis of bidirectional DC–DC converters for electric vehicles," *IEEE Trans. Ind. Appl.*, vol. 51, no. 4, pp. 3442–3452, Jul./Aug. 2015.
- [21] Y.-J. Lee, A. Khaligh, and A. Emadi, "Advanced integrated bidirectional AC/DC and DC/DC converter for plug-in hybrid electric vehicles," *IEEE Trans. Veh. Technol.*, vol. 58, no. 8, pp. 3970–3980, Oct. 2009.
- [22] O. C. Onar, J. Kobayashi, D. C. Erb, and A. Khaligh, "A bidirectional highpower-quality grid interface with a novel bidirectional noninverted Buck– Boost converter for PHEVs," *IEEE Trans. Veh. Technol.*, vol. 61, no. 5, pp. 2018–2032, Jun. 2012.